Dynamic Analysis of a Two-input Zeta Converter Topology for Modular Hybrid PV-Wind Microgrid System

Jane S. Salenga[1], Elmer R. Magsino[2]
[1]*De La Salle University*
Manila, Philippines
[2]*De La Salle University*
Manila, Philippines
[1]janesalenga@gmail.com
[2]elmer_magsino@yahoo.com

***Abstract* – This paper presents the dynamic modeling of a two-input Zeta converter topology using State-space averaging (SSA) technique. The modeling leads to a small-signal linear dynamic model of the multiple-input converter (MIC), from which the transfer functions used for feedback control design can be determined. To verify the accuracy of the obtained model, a two-input Zeta converter with inputs from PV array and wind turbine generation system (WTGS) is designed which can produce an output voltage of 350 Vdc and an output power of 1kW. A controller for this is designed based from the transfer functions derived from the dynamic analysis conducted. Simulation tests of the design are performed using blocks and component of Matlab/Simulink from its SimPower Systems Toolbox. Results are presented to verify the accuracy of the obtained model.**

***Keywords* – multiple-input converter, Zeta converter, DC-to-DC converter, microgrid system**

I. INTRODUCTION

The intermittent nature of renewable energy harvesting systems (REHS) such as photovoltaic arrays (PV arrays) and wind turbine generation systems (WTGS) had given rise to the development of a number of different topologies of DC-to-DC converters that can help maintain the output voltage of these systems at a constant level [1]. Nowadays, multiple-input converters (MIC) that can integrate various types of REHS using a single converter power stage are becoming popular [2][3][4][5]. PV arrays and WTGS are typically complementary to continuously provide energy to the load. This only means that the absence of light energy harvested by the PV arrays can be replaced by the presence of wind energy that can then be harvested by WTGS.

MIC topologies had been synthesized, analyzed, and evaluated in a few literatures [2][3][4][5][6]. However, none had focused on a multiple-input Zeta converter topology. An MI Zeta topology inherits the advantages of a single-input Zeta topology. This advantage includes the wide range of input voltage that it can handle since it can step up and down the input voltage. In addition to this, a Zeta converter can provide output voltage with positive polarity. This provides an advantage since most types of load requires this polarity of voltage. Also, a Zeta converter provides power factor correction which is a characteristic typically useful for highly reactive systems.

In this paper, a two-input Zeta converter which can integrate a PV array system and WTGS into a single power stage is studied. It is important to take note that although the focus of the study is only for a two-input Zeta, the study can easily be extended to three or more inputs Zeta converter. This topology provides potential modularity which means that its design can provide more flexible and scalable architecture. This also means that using this topology, multiple inputs of the converter can be replaced in a much easier way.

To determine the characteristics of the two-input Zeta, its dynamic modeling is implemented using State-space averaging (SSA) technique. A dynamic model of a converter provides information on its dynamic behavior and a basis for its feedback control design. SSA was chosen because of the inherit advantages pointed out in the dynamic modeling conducted for a single-input Zeta converter provided in [7]. To verify the validity of the obtained model, a two-input Zeta converter with its feedback controller is designed, implemented and simulated in Matlab/Simulink.

The paper is organized as follows. The SSA technique is reviewed in Section II. Modeling of the two-input Zeta converter using SSA technique is demonstrated in Section III. A design example is presented in IV. Simulation results are presented in Section V. And lastly, Section V gives the conclusion of the study.

II. OVERVIEW OF THE SSA TECHNIQUE

For a two-input DC-to-DC converter operating in Continuous Conduction Mode (CCM), there exist three power circuit states within one switching period, T. One is when MOSFET Q1 and Q2 are turned on for an interval

978-1-4799-8641-5/15/$31.00 ©2015 IEEE

d_2T, another is when MOSFET Q1 is still turned on while MOSFET Q2 is off for an interval $(d_1 - d_2)T$, and when both MOSFETs are off for an interval $(1 - d_1)T$, where d_1 and d_2 are the duty cycles of MOSFETs Q1 and Q2 and wherein d_1 is greater than d_2. The state-space equations for these three circuit states are:

$$\begin{cases} \frac{dx(t)}{dt} = \mathrm{A}_1 x(t) + \mathrm{B}_1 u(t) \\ y(t) = \mathrm{C}_1 x(t) + \mathrm{E}_1 u(t) \end{cases} \quad (1)$$

$$\begin{cases} \frac{dx(t)}{dt} = \mathrm{A}_2 x(t) + \mathrm{B}_2 u(t) \\ y(t) = \mathrm{C}_2 x(t) + \mathrm{E}_2 u(t) \end{cases} \quad (2)$$

$$\begin{cases} \frac{dx(t)}{dt} = \mathrm{A}_3 x(t) + \mathrm{B}_3 u(t) \\ y(t) = \mathrm{C}_3 x(t) + \mathrm{E}_3 u(t) \end{cases} \quad (3)$$

To find the averaged behavior of the converter over one switching period, (1), (2), and (3) are weighed average by the duty cycles as:

$$\begin{cases} \frac{dx(t)}{dt} = \mathrm{A}_\mathrm{S} x(t) + \mathrm{B}_\mathrm{S} u(t) \\ y(t) = \mathrm{C}_\mathrm{S} x(t) + \mathrm{E}_\mathrm{S} u(t) \end{cases} \quad (4)$$

where:

$$\begin{aligned} \mathrm{A}_\mathrm{S} &= \mathrm{A}_1 d_2 + \mathrm{A}_2(d_1 - d_2) + \mathrm{A}_3(1 - d_1), \\ \mathrm{B}_\mathrm{S} &= \mathrm{B}_1 d_2 + \mathrm{B}_2(d_1 - d_2) + \mathrm{B}_3(1 - d_1), \\ \mathrm{C}_\mathrm{S} &= \mathrm{C}_1 d_2 + \mathrm{C}_2(d_1 - d_2) + \mathrm{C}_3(1 - d_1), \\ \mathrm{E}_\mathrm{S} &= \mathrm{E}_1 d_2 + \mathrm{E}_2(d_1 - d_2) + \mathrm{E}_3(1 - d_1). \end{aligned}$$

Equation (4) is a non-linear continuous-time equation. It can be linearized by small-signal perturbation with x = X + $\tilde{\mathrm{x}}$, y = Y + $\tilde{\mathrm{y}}$, u = U + $\tilde{\mathrm{u}}$, and $d = D + \tilde{d}$, where the ~ symbol represents a small signal, and the capital letter a DC value. It should be noted that X >>$\tilde{\mathrm{x}}$, Y >>$\tilde{\mathrm{y}}$, U >>$\tilde{\mathrm{u}}$, and D >>$\tilde{d}$. The perturbation yields the stead-state and linear small-signal state-space equations in (5) and (6), respectively.

$$\begin{cases} \frac{d\mathrm{X}}{dt} = \mathrm{AX} + \mathrm{BU} = 0 \\ \mathrm{Y} = \mathrm{CX} + \mathrm{EU} \end{cases} \quad (5)$$

$$\begin{cases} \frac{d\tilde{x}(t)}{dt} = \mathrm{A}\tilde{x}(t) + \mathrm{B}\tilde{u}(t) + \mathrm{B}_\mathrm{d}\tilde{d}(t) \\ \tilde{y}(t) = \mathrm{C}\tilde{x}(t) + \mathrm{E}\tilde{u}(t) + \mathrm{E}_\mathrm{d}\tilde{d}(t) \end{cases} \quad (6)$$

where

$$\begin{aligned} \mathrm{A} &= \mathrm{A}_1 D_2 + \mathrm{A}_2(D_1 - D_2) + \mathrm{A}_3(1 - D_1), \\ \mathrm{B} &= \mathrm{B}_1 D_2 + \mathrm{B}_2(D_1 - D_2) + \mathrm{B}_3(1 - D_1), \\ \mathrm{C} &= \mathrm{C}_1 D_2 + \mathrm{C}_2(D_1 - D_2) + \mathrm{C}_3(1 - D_1), \\ \mathrm{E} &= \mathrm{E}_1 D_2 + \mathrm{E}_2(D_1 - D_2) + \mathrm{E}_3(1 - D_1), \\ \mathrm{B}_{\mathrm{d}1} &= (\mathrm{A}_2 - \mathrm{A}_3)X + (\mathrm{B}_2 - \mathrm{B}_3)U, \\ \mathrm{B}_{\mathrm{d}2} &= (\mathrm{A}_1 - \mathrm{A}_2)X + (\mathrm{B}_1 - \mathrm{B}_2)U, \\ \mathrm{E}_{\mathrm{d}1} &= (\mathrm{C}_2 - \mathrm{C}_3)X + (\mathrm{E}_2 - \mathrm{E}_3)U, \\ \mathrm{E}_{\mathrm{d}2} &= (\mathrm{C}_1 - \mathrm{C}_2)X + (\mathrm{E}_1 - \mathrm{E}_2)U. \end{aligned}$$

The steady-state solution of the converter can be found by solving (5) which gives:

$$\begin{cases} \mathrm{X} = -\mathrm{A}^{-1}\mathrm{BU} \\ \mathrm{Y} = (-\mathrm{CA}^{-1}\mathrm{B} + \mathrm{E})\mathrm{U} \end{cases} \quad (7)$$

The small-signal transfer function of the converter can be found by applying the Laplace transform to (5). In a matrix form, we get:

$$\begin{cases} \tilde{x}(s) = [(s\mathrm{I} - \mathrm{A})^{-1}\mathrm{B} \quad (s\mathrm{I} - \mathrm{A})^{-1}\mathrm{B}_{\mathrm{d}1} \quad (s\mathrm{I} - \mathrm{A})^{-1}\mathrm{B}_{\mathrm{d}2}] \begin{bmatrix} \tilde{u}(s) \\ \tilde{d}_1(s) \\ \tilde{d}_2(s) \end{bmatrix} \\ \tilde{y}(s) = [\mathrm{C}(s\mathrm{I} - \mathrm{A})^{-1}\mathrm{B} + \mathrm{E} \quad \mathrm{C}(s\mathrm{I} - \mathrm{A})^{-1}\mathrm{B}_{\mathrm{d}1} + \mathrm{E}_{\mathrm{d}1} \quad \mathrm{C}(s\mathrm{I} - \mathrm{A})^{-1}\mathrm{B}_{\mathrm{d}2} + \mathrm{E}_{\mathrm{d}2}] \begin{bmatrix} \tilde{u}(s) \\ \tilde{d}_1(s) \\ \tilde{d}_2(s) \end{bmatrix} \end{cases} \quad (8)$$

In DC-to-DC converters, the input variable $\tilde{\mathrm{u}}$ usually contains the input voltages, and load current. Hence, $\tilde{\mathrm{u}}$ is express as $\tilde{\mathrm{u}} = [u_1 \quad u_2]^{\mathrm{T}}$, the matrix B as $\mathrm{B} = [\mathrm{B}_{\mathrm{u}1} \quad \mathrm{B}_{\mathrm{u}2}]$, and the matrix E as $\mathrm{E} = [\mathrm{E}_{\mathrm{u}1} \quad \mathrm{E}_{\mathrm{u}2}]$. Therefore,

$$\begin{cases} \tilde{x}(s) = [(s\mathrm{I} - \mathrm{A})^{-1}\mathrm{B}_{\mathrm{u}1} \quad (s\mathrm{I} - \mathrm{A})^{-1}\mathrm{B}_{\mathrm{u}2} \quad (s\mathrm{I} - \mathrm{A})^{-1}\mathrm{B}_{\mathrm{d}1} \quad (s\mathrm{I} - \mathrm{A})^{-1}\mathrm{B}_{\mathrm{d}2}] \begin{bmatrix} \tilde{u}_1(s) \\ \tilde{u}_2(s) \\ \tilde{d}_1(s) \\ \tilde{d}_2(s) \end{bmatrix} \\ \tilde{y}(s) = [\mathrm{C}(s\mathrm{I} - \mathrm{A})^{-1}\mathrm{B}_{\mathrm{u}1} + \mathrm{E}_{\mathrm{u}1} \quad \mathrm{C}(s\mathrm{I} - \mathrm{A})^{-1}\mathrm{B}_{\mathrm{u}2} + \mathrm{E}_{\mathrm{u}2} \quad \mathrm{C}(s\mathrm{I} - \mathrm{A})^{-1}\mathrm{B}_{\mathrm{d}1} + \mathrm{E}_{\mathrm{d}1} \quad \mathrm{C}(s\mathrm{I} - \mathrm{A})^{-1}\mathrm{B}_{\mathrm{d}2} + \mathrm{E}_{\mathrm{d}2}] \begin{bmatrix} \tilde{u}_1(s) \\ \tilde{u}_2(s) \\ \tilde{d}_1(s) \\ \tilde{d}_2(s) \end{bmatrix} \end{cases} \quad (9)$$

For the sixth order converter, $(s\mathrm{I} - \mathrm{A})^{-1}\mathrm{B}_{\mathrm{u}1}$, $(s\mathrm{I} - \mathrm{A})^{-1}\mathrm{B}_{\mathrm{u}2}$, $(s\mathrm{I} - \mathrm{A})^{-1}\mathrm{B}_{\mathrm{u}3}$, $(s\mathrm{I} - \mathrm{A})^{-1}\mathrm{B}_{\mathrm{d}1}$, and $(s\mathrm{I} - \mathrm{A})^{-1}\mathrm{B}_{\mathrm{d}2}$ are the matrices that have six rows and one column. So the above equations can be extended into:

$$\begin{cases} \tilde{x}(s) = \begin{bmatrix} G_{vs1is1}(s) & G_{vs2is1}(s) & G_{d1is1}(s) & G_{d2is1}(s) \\ G_{vs1is2}(s) & G_{vs2is2}(s) & G_{d1is2}(s) & G_{d2is2}(s) \\ G_{vs1io}(s) & G_{vs2io}(s) & G_{d1io}(s) & G_{d2io}(s) \\ G_{vs1vc1}(s) & G_{vs2vc1}(s) & G_{d1vc1}(s) & G_{d2vc1}(s) \\ G_{vs1vc2}(s) & G_{vs2vc2}(s) & G_{d1vc2}(s) & G_{d2vc2}(s) \\ G_{vs1vco}(s) & G_{vs2vco}(s) & G_{d1vco}(s) & G_{d2vco}(s) \end{bmatrix} \begin{bmatrix} \tilde{u}_1(s) \\ \tilde{u}_2(s) \\ \tilde{d}_1(s) \\ \tilde{d}_2(s) \end{bmatrix} \\ \tilde{y}(s) = [G_{vs1vo}(s) \quad G_{vs2vo}(s) \quad G_{d1vo}(s) \quad G_{d2vo}(s)] \begin{bmatrix} \tilde{u}_1(s) \\ \tilde{u}_2(s) \\ \tilde{d}_1(s) \\ \tilde{d}_2(s) \end{bmatrix} \end{cases} \quad (10)$$

where

$G_{vs1is1} = [(s\mathrm{I} - \mathrm{A})^{-1}\mathrm{B}_{\mathrm{u}1}]_{11}$, $G_{vs2is1} = [(s\mathrm{I} - \mathrm{A})^{-1}\mathrm{B}_{\mathrm{u}2}]_{11}$, $G_{d1is1} = [(s\mathrm{I} - \mathrm{A})^{-1}\mathrm{B}_{\mathrm{d}1}]_{11}$, $G_{d2is1} = [(s\mathrm{I} - \mathrm{A})^{-1}\mathrm{B}_{\mathrm{d}2}]_{11}$, $G_{vs1is2} = [(s\mathrm{I} - \mathrm{A})^{-1}\mathrm{B}_{\mathrm{u}1}]_{21}$, $G_{vs2is2} = [(s\mathrm{I} - \mathrm{A})^{-1}\mathrm{B}_{\mathrm{u}2}]_{21}$, $G_{d1is2} = [(s\mathrm{I} - \mathrm{A})^{-1}\mathrm{B}_{\mathrm{d}1}]_{21}$, $G_{d2is2} = [(s\mathrm{I} - \mathrm{A})^{-1}\mathrm{B}_{\mathrm{d}2}]_{21}$, $G_{vs1io} = [(s\mathrm{I} - \mathrm{A})^{-1}\mathrm{B}_{\mathrm{u}1}]_{31}$, $G_{vs2io} = [(s\mathrm{I} - \mathrm{A})^{-1}\mathrm{B}_{\mathrm{u}2}]_{31}$, $G_{d1io} = [(s\mathrm{I} - \mathrm{A})^{-1}\mathrm{B}_{\mathrm{d}1}]_{31}$, $G_{d2io} = [(s\mathrm{I} - \mathrm{A})^{-1}\mathrm{B}_{\mathrm{d}2}]_{31}$, $G_{vs1vc1} = [(s\mathrm{I} - \mathrm{A})^{-1}\mathrm{B}_{\mathrm{u}1}]_{41}$, $G_{vs2vc1} = [(s\mathrm{I} - \mathrm{A})^{-1}\mathrm{B}_{\mathrm{u}2}]_{41}$, $G_{d1vc1} = [(s\mathrm{I} - \mathrm{A})^{-1}\mathrm{B}_{\mathrm{d}1}]_{41}$, $G_{d2vc1} = [(s\mathrm{I} - \mathrm{A})^{-1}\mathrm{B}_{\mathrm{d}2}]_{41}$, $G_{vs1vc2} = [(s\mathrm{I} - \mathrm{A})^{-1}\mathrm{B}_{\mathrm{u}1}]_{51}$, $G_{vs2vc2} = [(s\mathrm{I} - \mathrm{A})^{-1}\mathrm{B}_{\mathrm{u}2}]_{51}$, $G_{d1vc2} = [(s\mathrm{I} - \mathrm{A})^{-1}\mathrm{B}_{\mathrm{d}1}]_{51}$, $G_{d2vc2} = [(s\mathrm{I} - \mathrm{A})^{-1}\mathrm{B}_{\mathrm{d}2}]_{51}$, $G_{vs1vco} = [(s\mathrm{I} - \mathrm{A})^{-1}\mathrm{B}_{\mathrm{u}1}]_{61}$, $G_{vs2vco} = [(s\mathrm{I} - \mathrm{A})^{-1}\mathrm{B}_{\mathrm{u}2}]_{61}$, $G_{d1vco} = [(s\mathrm{I} - \mathrm{A})^{-1}\mathrm{B}_{\mathrm{d}1}]_{61}$, $G_{d2vco} = [(s\mathrm{I} - \mathrm{A})^{-1}\mathrm{B}_{\mathrm{d}2}]_{61}$, $G_{vs1vo} = C(s\mathrm{I} - \mathrm{A})^{-1}\mathrm{B}_{\mathrm{u}1} + E_{u1}$, $G_{vs2vo} = C(s\mathrm{I} - \mathrm{A})^{-1}\mathrm{B}_{\mathrm{u}2} + E_{u2}$, $G_{d1vo} = C(s\mathrm{I} - \mathrm{A})^{-1}\mathrm{B}_{\mathrm{d}1} + E_{d1}$, $G_{d2vo} = C(s\mathrm{I} - \mathrm{A})^{-1}\mathrm{B}_{\mathrm{d}2} + E_{d2}$.

III. MODELING OF THE TWO-INPUT ZETA CONVERTER BY SSA TECHNIQUE

A two-input Zeta converter shown in Fig. 1(a) is made of two MOSFET switches (Q_1 and Q_2), diodes (D_1 and D_2), three inductors (L_1, L_2, and L_O), and three capacitors (C_1, C_2, and C_O).

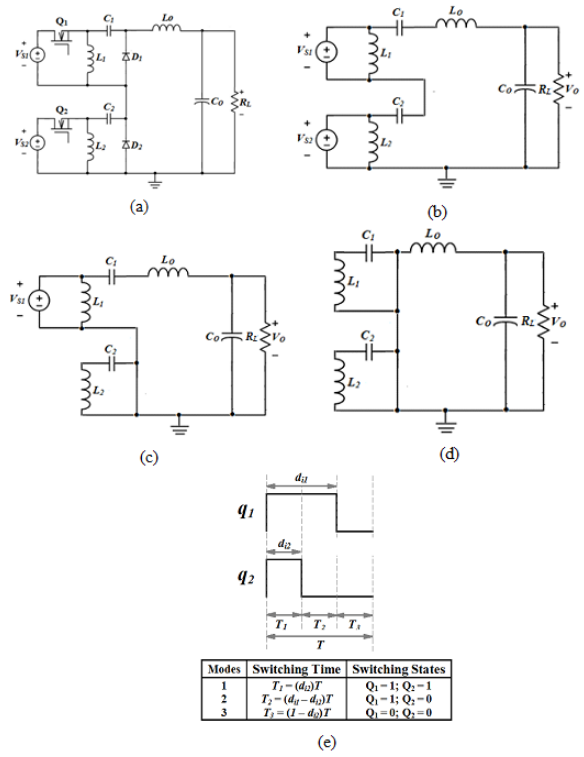

Figure 1: Operation of Two-input Zeta Converter: (a) the two-input Zeta converter configuration; (b) the two-input Zeta converter when both MOSFETs Q1 and Q2 are on; (c) the two-input Zeta converter when MOSFET Q1 is on while Q2 is off; (d) the two-input Zeta converter when both MOSFETs Q1 and Q2 are off; (d) switching waveforms

In continuous conduction mode (CCM), the number of operational modes of the converter is dependent on the status of the drive signals $q_1(t)$ and $q_2(t)$. One of the advantages of using this topology is that the simplified dynamic equations that we can derive from it are the same for all combinations of duty cycle values. That is, if we consider the two-input converter, when $D_1 > D_2$, $D_1 < D_2$, or $D_1 = D_2$. However, for brevity, the discussion focuses only to the case when $D_1 > D_2$. The gating signals $q_1(t)$ and $q_2(t)$ at this duty cycle combination is depicted in Fig. 1(e). From this correlation, the converter will operate in three circuit states which are illustrated in Fig. 1(b) to (c). The first circuit state exists when both Q_1 and Q_2 are turned on. During this interval d_2T, the currents through L_1, L_2, and L_O (as shown in Fig. 2) are supplied by V_{s2} and hence i_{L1}, i_{L2}, and i_{LO} increase linearly. This is called the charging interval. The charging interval continuous at the second circuit state but this time only currents through L_1 and L_2 increases as supplied by V_{S1}. During this interval $(d_1 - d_2)T$, Q_1 is still turned on while Q_2 is not. The third circuit state exists when both Q_1 and Q_2 are turned off. During this interval $(1 - d_1)T$, L_1 and L_O release the stored energy to C_O and the load. This interval is known as the discharging mode.

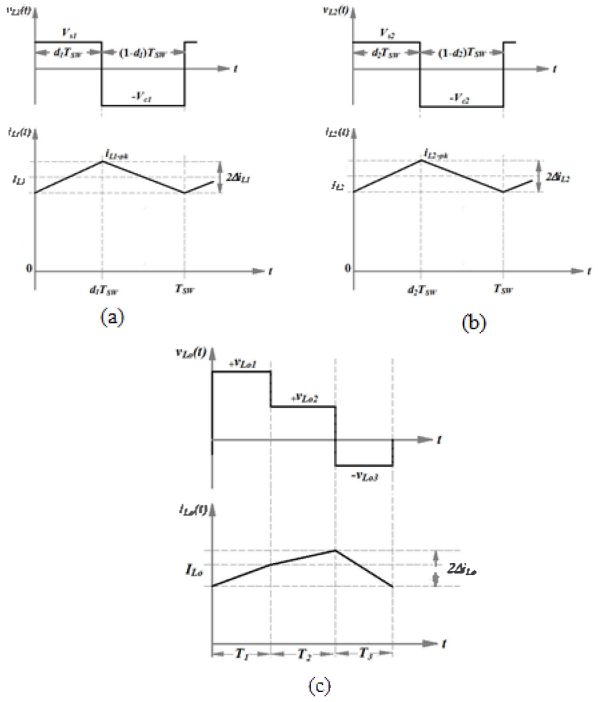

Fig. 2 Theoretical voltage and current waveforms in CCM of inductor (a) L_1; (b) L_2; (c) L_O.

A. *State-Space Description*

Following (1) and (2), the state-space equations of the two-input Zeta converter for the three states can be written from Fig. 1 (b), (c), and (d), given:

$$\begin{cases} L_1\dfrac{di_{L1}}{dt} = q_1V_{s1} + (1-q_1)v_{c1} \\ L_2\dfrac{di_{L2}}{dt} = q_2V_{s2} + (1-q_2)v_{c2} \\ L_O\dfrac{di_{LO}}{dt} = q_1V_{s1} - q_1v_{c1} + q_2V_{s2} - q_2v_{c2} - v_{co} \\ C_1\dfrac{dv_{c1}}{dt} = q_1i_{Lo} - (1-q_1)i_{L1} \\ C_2\dfrac{dv_{c2}}{dt} = q_2i_{Lo} - (1-q_2)i_{L2} \\ C_o\dfrac{dv_{co}}{dt} = i_{Lo} - \dfrac{v_{co}}{R_L} \\ v_O = v_{co} \end{cases} \tag{11}$$

It should be noted that q_1 and q_2 from equation (11) represents the switching states of MOSFETs Q_1 and Q_2; while, I_z represents the current across the load and may also be computed as $\frac{V_O}{R_L}$. From equations (5) and (6), the averaged matrices for the steady-state equations and the linear small-signal state-space equations are:

$$\mathrm{A}=\begin{bmatrix} 0 & 0 & 0 & \frac{(1-D_1)}{L_1} & 0 & 0 \\ 0 & 0 & 0 & 0 & \frac{(1-D_2)}{L_2} & 0 \\ 0 & 0 & 0 & \frac{-D_1}{L_O} & \frac{-D_2}{L_O} & \frac{-1}{L_O} \\ \frac{-(1-D_1)}{C_1} & 0 & \frac{D_1}{C_1} & 0 & 0 & 0 \\ 0 & \frac{-(1-D_2)}{C_2} & \frac{D_2}{C_2} & 0 & 0 & 0 \\ 0 & 0 & \frac{1}{C_O} & 0 & 0 & \frac{-1}{C_O R_L} \end{bmatrix} \quad (12)$$

$$\mathrm{B}=\begin{bmatrix} \frac{D_1}{L_1} & 0 \\ 0 & \frac{D_2}{L_2} \\ \frac{D_1}{L_O} & \frac{D_2}{L_O} \\ 0 & 0 \\ 0 & 0 \\ 0 & 0 \end{bmatrix} \quad (13)$$

$$\mathrm{C}=[0 \quad 0 \quad 0 \quad 0 \quad 0 \quad 1] \quad (14)$$

$$\mathrm{E}=[0 \quad 0] \quad (15)$$

$$\mathrm{B_{d1}}=\begin{bmatrix} \frac{V_{S1}}{L_1(1-D_1)} \\ \frac{D_2 V_{S2}}{L_2(1-D_2)} \\ \frac{V_{S1}}{L_1}+\frac{D_1 V_{S1}}{L_O(1-D_1)}+\frac{D_2 V_{S2}}{L_O(1-D_2)} \\ \frac{D_1 V_{S1}+D_2 V_{S2}-D_1 D_2 V_{S1}-D_1 D_2 V_{S2}}{C_1 R_L(1-D_1)^2(1-D_2)} \\ \frac{D_1 V_{S1}+D_2 V_{S2}-D_1 D_2 V_{S1}-D_1 D_2 V_{S2}}{C_2 R_L(1-D_2)^2(1-D_1)} \\ 0 \end{bmatrix} \quad (16)$$

$$\mathrm{B_{d2}}=\begin{bmatrix} 0 \\ \frac{V_{S2}}{L_2} \\ \frac{V_{S2}}{L_O}-V_{S1}\left(\frac{1}{L_1}-\frac{1}{L_O}\right) \\ 0 \\ 0 \\ 0 \end{bmatrix} \quad (17)$$

$$\mathrm{E_d}=[0] \quad (18)$$

B. *Steady-State Equations*

Given the averaged matrices (12) to (18), the steady-state solution of the converter can be obtained from (7):

$$\begin{cases} \begin{bmatrix} I_{L1} \\ I_{L2} \\ I_{Lo} \\ V_{C1} \\ V_{C2} \\ V_{Co} \end{bmatrix} = \begin{bmatrix} \frac{D_1^2}{R_L(1-D_1)^2} & \frac{D_1 D_2}{R_L(1-D_1)(1-D_2)} \\ \frac{D_1 D_2}{R_L(1-D_1)(1-D_2)} & \frac{D_2^2}{R_L(1-D_2)^2} \\ \frac{D_1}{R_L(1-D_1)} & \frac{D_2}{R_L(1-D_2)} \\ 0 & \frac{-D_2}{(1-D_2)} \\ \frac{D_1}{1-D_1} & \frac{D_2}{1-D_2} \end{bmatrix} \begin{bmatrix} V_{S1} \\ V_{S2} \end{bmatrix} \quad (18) \\ V_O = V_{S1}\left(\frac{D_1}{1-D_1}\right)+V_{S2}\left(\frac{D_2}{1-D_2}\right) \end{cases}$$

From the equation for V_O in (18), we can find that the output voltage of the two-input Zeta converter is simply equivalent to the sum of two single-input Zeta converters.

D. *Finding the Transfer Functions*

From (10), there are altogether twenty-eight transfer functions that can be determined. However, only a few of them are significant for feedback control design purpose. These transfer functions include the duty ratios-to-output voltage transfer functions which can be derived using the following equations:

$$G_{d1vo}=C(\mathrm{sI}-\mathrm{A})^{-1}\mathrm{B_{d1}}+E_{d1} \quad (19)$$

$$G_{d2vo}=C(\mathrm{sI}-\mathrm{A})^{-1}\mathrm{B_{d2}}+E_{d2} \quad (20)$$

and the input voltages-to-output voltage transfer functions which can be derived using the following equations:

$$G_{vs1vo}=C(\mathrm{sI}-\mathrm{A})^{-1}\mathrm{B_{u1}}+E_{u1} \quad (21)$$

$$G_{vs2vo}=C(\mathrm{sI}-\mathrm{A})^{-1}\mathrm{B_{u2}}+E_{u2} \quad (22)$$

The actual equations are somewhat complicated are no longer presented here because of space limitations. However, to make the derivation easier, a MATLAB code is created from the derived equations presented above. (See Appendix A)

IV. DESIGN EXAMPLE

A two-input Zeta converter was designed to output 350 Vdc at a 122.5-Ω load resistance and 1 kW output power. Using steady-state analysis, the following values of parameters can be derived: L_1 = 870 uH, L_2 = 4433 uH, L_O = 4183.3 uH, C_1 = 2.85 uF, C_2 = 0.47 uF and C_O = 0.05uF. Using these values of converter parameters, the duty ratios-to-output voltage and input voltages-to-output voltage transfer functions were derived using the analysis presented in this paper. A controller for the two-input converter was then designed with the help of MATLAB SISOTOOL. When the duty cycle of D_1 is used to maintain the output voltage at 350 Vdc under varying input voltages and load and while duty ratio D_2 varies, the resulting compensator transfer function is as follows:

$$G_C = 20\left(\frac{1.7x10^{-7}s^2+1.7x10^{-2}s+1}{1x10^{-2}s^2+2x10^{-1}+1}\right)$$

The complete design was created in MATLAB/Simulink to determine the validity of the dynamic analysis conducted. Six sets of values of input voltages, duty cycle D_2 and load were used to test the design. They are as follows:

Condition 1:
V_{S1} = 100 Vdc; V_{S2} = 400 Vdc; D_2 = 0.2; R_L = 122.5-Ω
Condition 2:
V_{S1} = 400 Vdc; V_{S2} = 100 Vdc; D_2 = 0.2; R_L = 122.5-Ω
Condition 3:
V_{S1} = 400 Vdc; V_{S2} = 100 Vdc; D_2 = 0.6; R_L = 122.5-Ω
Condition 4:
V_{S1} = 400 Vdc; V_{S2} = 100 Vdc; D_2 = 0.6; R_L = 122.5-Ω
Condition 5:
V_{S1} = 400 Vdc; V_{S2} = 100 Vdc; D_2 = 0.6; R_L = 100-Ω
Condition 6:
V_{S1} = 100 Vdc; V_{S2} = 400 Vdc; D_2 = 0.2; R_L = 100-Ω.

V. SIMULATION RESULTS

The simulation results for Condition 1 to 6 are given in Fig. 3 to 8. From these figures we can see that under all the conditions cited, the output voltage settled at 350 Vdc in approximately 60 milliseconds after the input voltages were applied. Results also showed that power was maintained at 1 kW for conditions 1 to 4. On the other hand, the output power changed to approximately 1.2 kW when the load changed to 100-Ω in conditions 5 and 6. These results simply proves that using the converter transfer functions derived from the dynamic analysis conducted in this study, a controller for the two-input converter can be designed to maintain the output voltage of the two-input Zeta converter at a constant level under varying input voltages and load. Thus, providing the validity of the dynamic analysis conducted.

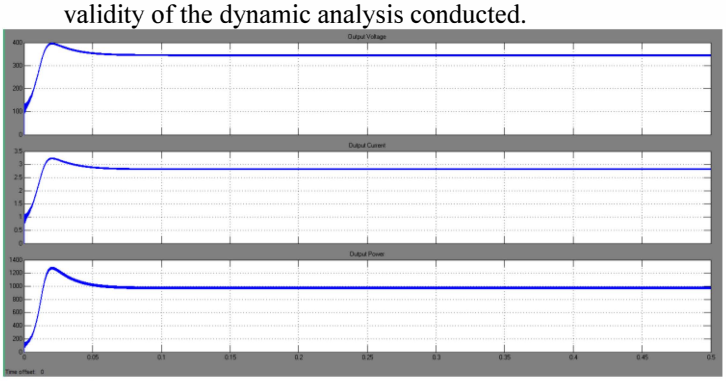

Figure 3: Converter Output Voltage (Upper), Converter Output Current (Middle), and Converter Output Power (Lower) for Condition 1.

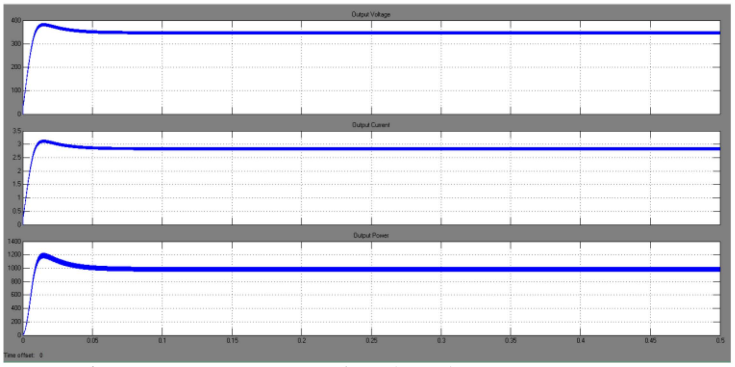

Figure 4: Converter Output Voltage (Upper), Converter Output Current (Middle), and Converter Output Power (Lower) for Condition 2.

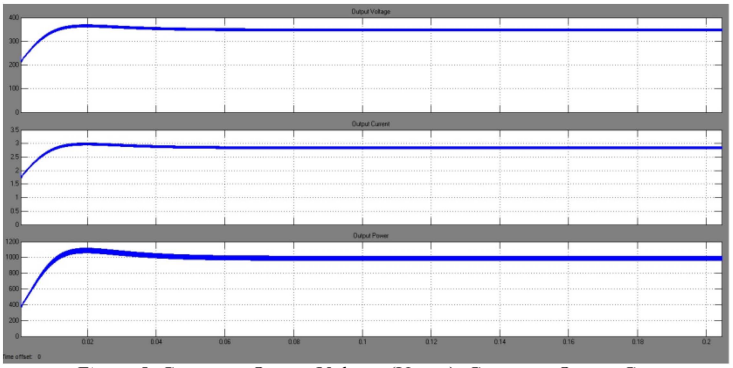

Figure 5: Converter Output Voltage (Upper), Converter Output Current (Middle), and Converter Output Power (Lower) for Condition 3.

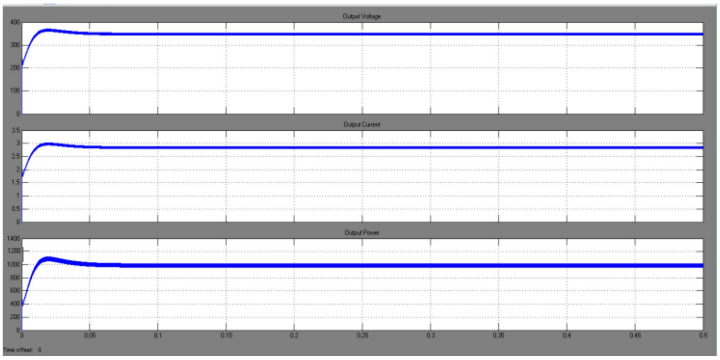

Figure 6: Converter Output Voltage (Upper), Converter Output Current (Middle), and Converter Output Power (Lower) for Condition 4.

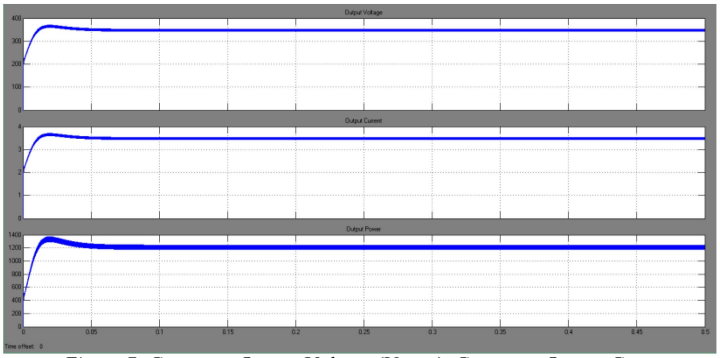

Figure 7: Converter Output Voltage (Upper), Converter Output Current (Middle), and Converter Output Power (Lower) for Condition 5.

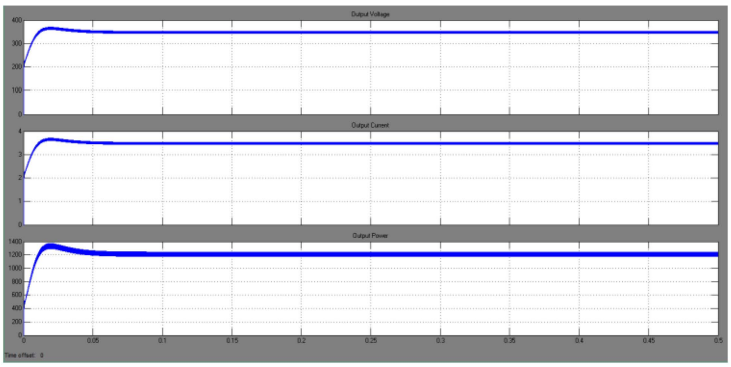

Figure 7: Converter Output Voltage (Upper), Converter Output Current (Middle), and Converter Output Power (Lower) for Condition 6.

VI. CONCLUSIONS

In this paper, the dynamic analysis of a two-input Zeta DC-to-DC converter has been performed using State-space Averaging (SSA) technique. The results yield an insight into the steady-state and small-signal dynamic properties of the converter. To provide a basis for the controller design, relevant transfer functions were derived and were used to design a controller that can maintain its output under varying levels of the input voltages and load. The design was implemented in MATLAB/Simulink, and results were shown to validate the small-signal dynamic model of the two-input Zeta converter.

REFERENCES

[1] Badejani, M.M., Masoum, M.A.S., & Kalantar, M., "Optimal design and modeling of stand-alone hybrid PV-wind systems", *Australasian Universities Power Engineering Conference, 2007 (AUPEC 2007),* pp. 1-6, 9-12 December 2007, doi: 10.1109/AUPEC.2007.4548134.

[2] Ramya, S. & Manokaran, T., "Analysis and design of multi input DC-DC converter for integrated wind PV cell renewable energy generated system", International Journal of Recent Technology in Engineering, ISSN: 2277-3878 Volume 1, Issue 5, November, 2012.

[3] Chitra, L., Nandhini, M., & Karpagam, M., "Model of multiple input boost converter for renewable energy system using Matlab/Simulink", *International Journal of Scientific & Engineering Research,* Volume 4, Issue3, March-2013, ISSN 2229-5518.

[4] Saravanan, S., Sureshkumar, A., & Thangavel, S., "A New Topology of Multiple-Input Converter with Embedded Controller Based Power Management", *International Journal of Engineering and Advanced Technology (IJEAT),* ISSN: 2249 – 8958, Volume-2, Issue-4, April 2013.

[5] Butterfield, B., Anwari, M. & Taufik, M. "Modeling and simulation of multiple-input converter system with equally drawn source power", *2009 Third Asia International Conference on Modelling & Simulation,* April, 2009. DOI 10.1109/AMS.2009.84.

[6] A. Khaligh, J. Cao, and Y.-J. Lee, "A multiple-input dc–dc converter topology," *IEEE Trans. Power Electron.*, vol. 24, no. 3, pp. 862–868, Mar. 2009.

[7] Vuthchhay, E. and Bunlaksananusorn, C., "Dynamic Modeling of a Zeta Converter with State-Space Averaging Technique," *5th International Conference on Electrical Engineering/Electronics, Computer, Telecommunications and Information Technology,* Volume 2, pp. 969 – 972, May 14 – 17, 2008.

APPENDIX A

MATLAB Code to Derive Converter Transfer Functions

```
clear all
clc
syms D1 D2 L1 L2 Lo C1 C2 Co RL Vs1 Vs2 s

A = [0 0 0 (1-D1)/L1 0 0; 0 0 0 0 (1-D2)/L2 0; 0 0 0 -D1/Lo -D2/Lo -
1/Lo; -(1-D1)/C1 0 D1/C1 0 0 0; 0 -(1-D2)/C2 D2/C2 0 0 0; 0 0 1/Co 0 0 -
1/(Co*RL)];
B = [D1/L1 0; 0 D2/L2; D1/Lo D2/Lo; 0 0; 0 0; 0 0];
C = [0 0 0 0 0 1];
A1 = [0 0 0 0 0 0; 0 0 0 0 0 0; 0 0 0 -1/Lo -1/Lo -1/Lo; 0 0 1/C1 0 0 0; 0 0
1/C2 0 0 0; 0 0 1/Co 0 0 -1/(Co*RL)];
A2 = [0 0 0 0 0 0; 0 0 0 0 0 0; 0 0 0 -1/Lo -1/Lo -1/Lo; 0 0 1/C1 0 0 0; 0 0
1/C2 0 0 0; 0 0 1/Co 0 0 -1/(Co*RL)];
A3 = [0 0 0 1/L1 0 0; 0 0 0 0 1/L2 0; 0 0 0 0 0 -1/Lo; -1/C1 0 0 0 0 0; 0 -
1/C2 0 0 0 0; 0 0 1/Co 0 0 -1/(Co*RL)];
B1 = [1/L1 0; 0 1/L2; 1/Lo 1/Lo; 0 0; 0 0; 0 0];
B2 = [1/L1 0; 0 0; 1/L1 0; 0 0; 0 0; 0 0];
B3 = [0 0; 0 0; 0 0; 0 0; 0 0; 0 0];
E = [0 0];
U = [Vs1; Vs2];
invA = inv(A);
X = -invA*B*U;
Y = -(C*invA*B+E)*U;
Bd1 = (A2 - A3)*X + (B2 - B3)*U;
Bd2 = (A1 - A2)*X + (B1 - B2)*U;
sI = [s 0 0 0 0 0;0 s 0 0 0 0;0 0 s 0 0 0;0 0 0 s 0 0;0 0 0 0 s 0;0 0 0 0 0 s];
sIinv = inv(sI-A);
Bu1 = [D1/L1; 0; D1/Lo; 0 ; 0 ; 0];
Bu2 = [0; D2/L2; D2/Lo; 0; 0; 0];
Gvs1vco = C*sIinv*Bu1;
Gvs1vco_simp = simplify(Gvs1vco)
Gvs2vco = C*sIinv*Bu2;
Gvs2vco_simp = simplify(Gvs2vco)
Gd1vco = C*sIinv*Bd1;
Gd1vco_simp = simplify(Gd1vco)
Gd2vco = C*sIinv*Bd2;
Gd2vco_simp = simplify(Gd2vco)
```

APPENDIX B

Two-input Zeta Converter Simulink Model